16TH EUROPEAN CONFERENCE ON EARTHQUAKE ENGINEERING THESSALONIKI 18 - 21 JUNE 2018

HYBRID-SOURCE STRONG-MOTION ATTENUATION MODEL FOR COLOMBIA

Gabriel A. BERNAL[1], Omar-Dario CARDONA[2]

ABSTRACT

Strong motion modeling from kinematic source models can be divided into three main approaches: integral, composite and stochastic. In the integral approach, the propagation of the rupture is assumed to be a k-square pulse. This approach appropriately represents the low frequency regions of the Fourier amplitude spectrum of the strong motion, mainly dominated by the source scaling. Although on a large scale the occurrence of rupture can be considered to follow a uniform pattern as the integral approach considers, on a smaller scale the rupture propagates in a chaotic manner. This condition is more appropriately modeled with the composite approach, where it is considered that the rupture zone is formed by a series of seismic sub-sources where the rupture occurs randomly. Although this approach leads to better approximations in the high frequency region of the Fourier spectrum, it does not adequately represent the low frequency region. Finally, the stochastic approach consists in estimating the Fourier amplitude spectrum by means of a source amplitude spectrum model, and stochastically generating the phase spectrum. In this study, a hybrid source model is used, combining the approaches mentioned above in the kinematic simulation of the rupture. A new attenuation model based on the hybrid Fourier amplitude spectrum formulation, calibrated for the Colombian territory, is presented, which allows the estimation of complete accelerograms at any location in the territory. The accelerograms are generated as a function of magnitude and distance, and additionally by the three-dimensional geometry of the source plane and a geometric limitation of the area of rupture. The occurrence of an earthquake is then modeled by aggregation of the dislocation into a collection of individual sub-sources which together represent the zone of complete rupture. The total dislocation is evenly distributed among all sub-sources, so that the earthquake's total seismic moment is conserved. In the calculation site, all the synthetic accelerograms contributed by the collection of sub-sources are integrated, each generated with the portion of the seismic moment that corresponds to it, and with different arrival times. Possible engineering applications of the proposed model are discussed.

Keywords: Strong motion; Attenuation; Simulated accelerograms; Source model

1. INTRODUCTION

Strong motion estimation is one of the most important aspects for seismic hazard modeling. Usually, this estimation is performed using attenuation functions or laws, also known as Ground Motion Prediction Equations (GMPE), which calculate the probability distribution of the acceleration (among other strong motion parameters) associated with the occurrence of an earthquake with known magnitude and distance. For several decades, seismic engineering and seismology have faced the strong motion estimation problem, developing a variated scientific literature, which includes multiple proposed solutions. This paper presents an alternative approach, which has also been studied in the past mainly in seismology, for the solution of the strong motion attenuation problem.

In the probabilistic assessment of seismic hazard, the intensity of strong motion is modeled as a random variable to rationally incorporate uncertainty associated with hazard estimation. In the common practice of seismic engineering, the attention is focused on the estimation of motion parameters of maximum amplitude (PGA, PGV, PGD), as well as the ordinates of the response

[1] Technical Manager, Ingeniar: Risk Intelligence Ltda., Bogotá D.C., Colombia, gabernal@ingeniar-risk.com
[2] Associated Professor, Universidad Nacional de Colombia, Manizales, Colombia, odcardonaa@unal.edu.co

spectrum. It is usual to represent strong motion parameters as random variables fitted to lognormal distributions, with probability moments defined by attenuation functions. The attenuation functions must represent adequately the transformation process that seismic waves suffer as they transit the earth's crust. These processes are associated to the kinetic energy losses mainly due to the wave front's movement and spread, and the anelasticity of the medium. Recently, a numerous variety of attenuation models have been developed, mainly based on historic data of motion recorded in accelerograph stations. From regressions on available data, it is possible to establish trends and dispersion of the motion intensities as a function of the seismic magnitude and source-site distance.

For the strong motion estimation problem, the attenuation functions (GMPEs) provide an important method for direct application; however, they are not the only usable approach. The simulation of seismograms and accelerographs from kinematic models of seismic sources is a growing and promising research field for the synthesis of complex expressions of strong motion. It is totally based on the understanding of the physical processes that control the problem and adjusted to the available accelerograph data. The simulation of accelerographs from source models can be performed using multiple methodologies, which can be grouped in three main approaches: integral, composite and stochastic.

Recent research has developed methodologies for the kinematic solution for the displacement of a seismic source and the radiated stress field after the occurrence of an earthquake. Seismological theory states that the strong motion associated to shear dislocation is defined by the representation theorem as follows:

$$u(r,t) = \iint_{\Sigma} G_{pq}(r,t,\xi) \cdot m_{pq}(t,\xi) d\Sigma \tag{1}$$

where, u is the displacement at point r, due to shear dislocation in Σ, at time t and observation point at ξ. G is the Green's tensor, and m is the moment tensor density, for the different pairs p-q that cause dislocation in the focal mechanism. The displacement's field solution, defined by the representation theorem, is possible under the acceptance of some assumptions and simplifications (more details in Aki and Richards 2002). The direct application of the analytical solution for the radiated displacement field from a seismic source constitutes the integral kinematic solution approach, which requires geometrical and kinematic source models, as well as the solution of Green's functions or the application of ray theory to simulate the transit of seismic waves through the earth's crust.

Although the representation theorem provides an adequate theoretical framework for the study of strong motion attenuation and allows the appropriate simulation of low-frequency motion, it has been shown that this formulation is not convenient for high-frequency motion simulation due to is high computational requirements. For this reason, composite source models have emerged, where the fault plane is discretized in a collection of sub-sources, each one with a fraction of the total seismic moment of the earthquake; assuming that the rupture occurs in a chaotic and disorganized manner among the collection of sub-sources. This approach allows the appropriate reproduction of the natural randomness of the high-frequency motion, with weakness in the estimation of low-frequency motion, mainly due to the incoherent aggregation of the total motion.

Finally, Boore (1983) proposed an alternative methodology based on the estimation of the Fourier amplitude spectrum by the application of a point source model with known seismic moment and hypocentral distance, and the modification of the mentioned amplitude spectrum with a gaussian noise signal to include randomness (which is equivalent to randomly simulate the phases spectrum). This methodology constitutes the stochastic approach. Several authors have applied the mentioned approaches to simulate accelerograms (see Boore 1983; Mai and Beroza 2003; Gallovic and Brokesova, 2004 and 2007; Özel et al. 2011).

In this work, a hybrid approach to simulate accelerographs is proposed. The source is defined as a plane immerse in an isotropic and homogeneous media. This plane is defined by the three fundamental direction components of source motion: dip δ, strike ϕ_s and rake λ. Figure 1 shows the general geometry of the fault plane on the footwall. It is also shown the reference coordinate system, where north is the *x* coordinate to ensure that the z-axes is positive in depth.

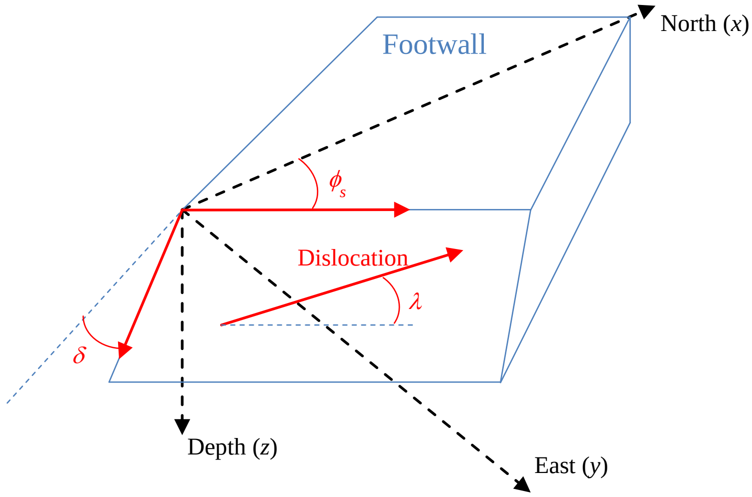

Figure 1. Parameters definition for the fault plane orientation (Adapted from Aki and Richards 2002).

2. SOURCE GEOMETRY MODEL

As mentioned before, this work formulates a hybrid source model, which with some simplifications, will allow to estimate complete accelerograms to assess seismic hazard, risk and structural damage. The source geometry is defined as a function of its orientation parameters, as shown in Figure 1. Within this fault plane, the hypocenter with coordinates x_h, y_h, z_h is localized where the energy associated with a seismic dislocation of magnitude Δu is concentrated. The first step consists in defining the rupture area after the occurrence of an earthquake, of known magnitude M_w, in the fault plane. In this work, the rupture area *(A)* is estimated following Singh et al. (1980):

$$\log(A) = M_w - 4 \tag{2}$$

Once the rupture area is calculated, a rectangle with that area is defined within the fault plane. The proportion of the rectangle sides is establish using a factor $\phi = \left(1+\sqrt{5}\right)/2$. The rectangle sides are determined in a way to preserve the total rupture area. The selection of a rectangular rupture area and the sides ratio was completely arbitrary; therefore, further research is needed to understand its incidence on the final result and to include complex rupture geometries to the model. At this point, it is convenient to define a local coordinate system on the fault plane that is associated with the rupture zone. As shown in Figure 2, the strike direction is coordinate *L* and the dip direction is coordinate *W*, locating the origin at the top-left corner of the rupture rectangle, and the hypocenter in the centroid of the plane. This is an arbitrary decision that also needs further research. It should be noted that for high magnitude and shallow earthquakes, the rupture area can be extended above surface, which is impossible. If such situation happens, the rectangle is displaced downwards until an appropriate location is reached. In the event of exceedance of the global size of the fault plane (due to restrictions associates with the geometry of seismic sources within a particular hazard model), the rectangle's side ratio is modified until the total rupture area is located within the fault boundaries.

The rupture area is oriented according to the rake λ direction. The scope of this work considers 3 possible rake directions, which are associated to different types of the focal mechanism: normal fault (λ = -π/2); reverse fault (λ = π /2); strike-slip fault (λ = 0). Therefore, for this research the variability of λ is limited to the mentioned cases. Nevertheless, the inclusion of the rake angle λ in the coordinate transformation from the rupture plane to the cartesian system is simple; therefore, the expansion of the proposed model to consider further rake angles is relatively straightforward.

Next, the rupture area is subdivided in a collection of rectangular sub-sources (which maintain the same aspect ratio as the original rectangle), following the fundamental concept of the composite seismic source approach. This discretization is done in terms of the observer in relation to the source-plane. The location of the observer is important because, if it is too close, the source must be considered as a finite source; otherwise, if the observer is at a greater distance from the plane-source, source can be considered as a point source. Both situations are simulated following the same methodology of the hybrid source model. The number of sections, in which is divided each side of the source's rupture area, is defined as:

$$N = \mathrm{int}\left(\frac{A}{\max\left(R_{Hyp} - r_e, 0\right) + 0.1}\right) + 1 \qquad (3)$$

where R_{Hyp} is the hypocentral distance and r_e is the equivalent radius of the rupture area (the resulting radius of a circle with area A). Note that as the hypocentral distance increases, associated to the rupture's size, the division number decreases until $N=1$ for very large distances. By contrast, if the hypocentral distance is very small in relation to the rupture's size, the division number is N = int(10A)+1. In this way, as A increases N increases too, which is consistent with the needs to subdivide larger areas in a larger number of sub-sources.

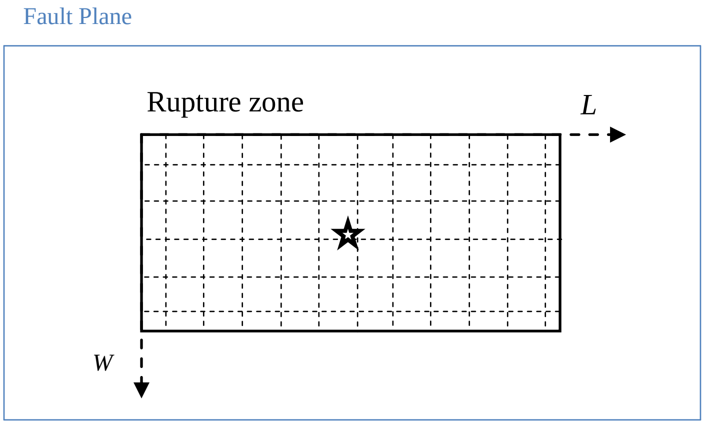

Figure 2. Rupture zone in the fault plane and L-W coordinated system. The star shows the location of the hypocenter. Note that the rupture area is subdivided in smaller regions.

3. DISLOCATION IN EACH SUBSOURCE

The magnitude of the dislocation Δu is proportional to the total seismic moment of the earthquake (*Mo):*

$$M_0 = \Delta u \cdot \mu \cdot A \qquad (4)$$

The total seismic moment is determined from the earthquake magnitude by the application of the moment magnitude definition by Hanks and Kanamori (1979):

$$M_W = 2/3 \log\left(M_0\right) - 10.7 \qquad (5)$$

Given the proportionality between the seismic moment and the total dislocation, a portion of the seismic moment is assigned to each sub-source in a way that, collectively, the total dislocation Δu is conserved.

$$\Delta u = \frac{\sum M_{0i}}{\mu A} \tag{6}$$

where M_{0i} is the portion of the assigned seismic moment to each sub-source i. The distribution of the seismic moment can be performed in many ways. In this work, the total seismic moment was assigned uniformly in all the sub-sources ($M_{0i} = M_0/N$ for all the sub-sources). However, due to the mathematical construction presented here, the incorporation of complex dislocation models in the future is relatively straightforward. Such models might consider the variability of asperities within fault, as well as the time that each dislocation takes in each sub-source. As reference, the reader can consult the stochastic dislocation models proposed by Mai and Beroza (2003), Gallovic and Brokesova (2004, 2007) and Özel et al. (2011).

4. DISPLACEMNT SPECTRUM RADIATED BY EACH SUB-SOURCE

The radiated displacement field from a source can be determined using the integral simulation approach, as explained above. The analytic solution for the Fourier amplitude spectrum of displacements was proposed by Aki in 1967, for a shear dislocation in a homogeneous and isotropic media. These formulations allow the definition of the strong motion generated by point seismic sources (i.e. where the distance to the observer is several times greater than the rupture's size). Since, in our approach the seismic source rupture's area is subdivided in an appropriate number of sub-sources (see Figure 2), it is possible to simulate each sub-source as a point source. The Fourier amplitude spectrum of acceleration $A(f,R_i,M_{0i})$, radiated from the sub-source i, assuming a source model ω^{-2}, can be written as:

$$A(f,R_i,M_{0i}) = C \cdot S(f,M_{0i}) \cdot G(R_i) \cdot F_Q(f,R_i) \cdot F_\kappa(f,R_i) \tag{7}$$

where f is the frequency, R_i is the hypocentral distance of sub-source i, and M_{0i} is its seismic moment. C is a constant related to the waves transit media, $S(f,M_{0i})$ is the source spectrum, $G(R_i)$ is the parameter of geometric propagation, $F_Q(f, R_i)$ is the anelasticity filter and $F_\kappa(f, R_i)$ is the local attenuation filter or kappa filter. The constant parameter is

$$C = \frac{R_{\theta\phi}(2\pi)^2 F \cdot P \cdot A_{up}}{4\pi\rho\beta^3} \tag{8}$$

where $R_{\theta\phi}$ is the radiation pattern, F is a free surface amplification factor, P is a partition factor of two orthogonal components of energy, ρ is the media density and β is its shear wave velocity. A_{up} is a correction factor for the amplification induced in S waves as they propagate upwards through material layers with decreasing shear-waves velocity (Boore 1986). Despite the frequency dependence, A_{up} is approximately 2 for f >1Hz. In this work the assumption is A_{up} = 2 for all the frequencies. The source parameter, for a source ω^{-2}, is defined as (Brune 1970):

$$S(f,M_{0i}) = \frac{M_{0i} \cdot f^2}{1+\left(\frac{f}{f_c}\right)^2}; \quad f_c = 4.9 \cdot 10^6 \beta \sqrt[3]{\frac{\Delta\sigma}{M_{0i}}} \tag{9}$$

where $\Delta\sigma$ is the stress drop and f_c is the corner frequency. The geometric propagation parameter:

$$G(R_i)=\begin{cases}1/R_i & for\ R_i \le R_x \\ 1/\sqrt{R_i \cdot R_x} & for\ R_i > R_x\end{cases} \tag{10}$$

This parameter explains the predominance of the body-waves in the propagation when $R \le R_x$, and surface waves when $R > R_x$. Hence, R_x is the distance at which the change of predominant waves is expected. Usually, surface waves are predominant for hypocentral distances higher than 100 km. The anelasticity filter is:

$$F_Q(f, R_i) = \exp\left(\frac{-\pi f R_i}{\beta Q(f)}\right) \tag{11}$$

where $Q(f)$ is the rock's quality factor Q (Knopoff, 1964) that is frequency-dependent. In this work, the dependency of Q and frequency is assumed as $Q = Q_0 f^{\varepsilon}$, which is a general version of the function assumed by several authors (see, for example: Castro et al. 1990; Ordaz and Singh 1992; Atkinson 1995; Tavaloki and Pezeshk 2005; Singh et al. 2007; Hassani et al. 2011). The local attenuation filter (or kappa filter) is:

$$F_\kappa = \exp(-\pi f \kappa) \tag{12}$$

The local attenuation filter is associated to the fact that the higher amplitude frequency attenuates faster than predicted because of anelasticity and geometric attenuation. This is caused mainly due to the conditions of surface proximity, which can vary from location to location. This filter accounts the spectrum amplitude reduction for $f > f_{max}$, where f_{max} is the frequency introduced by Hanks in 1982. Applying the abovementioned definitions on equation 7, for $R \le R_x$ (predominance of body-waves), the following is obtained:

$$A(f, R_i, M_{0i}) = C \cdot \frac{M_{0i} \cdot f^2}{1+\left(\frac{f}{f_c}\right)^2} \cdot \frac{1}{R_i} \cdot \exp\left(\frac{-\pi f R_i}{\beta Q_0 f^{\varepsilon}}\right) \cdot \exp(-\pi f \kappa) \tag{13}$$

and for $R > R_x$ (predominance of surface waves):

$$A(f, R_i, M_{0i}) = C \cdot \frac{M_{0i} \cdot f^2}{1+\left(\frac{f}{f_c}\right)^2} \cdot \frac{1}{\sqrt{R_i \cdot R_x}} \cdot \exp\left(\frac{-\pi f R_i}{\beta Q_0 f^{\varepsilon}}\right) \cdot \exp(-\pi f \kappa) \tag{14}$$

In this work, the values of the seismic parameters that define the source spectrum are assigned according to the proposal by Bernal (2014), and Bernal and Cardona (2015), for their PGA attenuation model of intraplate source: $\Delta\sigma$ = 236 bar, Q_0=723, ε = 0.9, κ = 0.0333, $R_{\theta\phi}$=0.642, R_x = 100 Km, ρ = 2.8 Ton/m3 y β = 3.5 Km/s. These parameters were defined by a calibration methodology of the source spectrum model against the accelerograph data of the National Accelerograph Network of Colombia (RNAC); therefore, the mentioned parameters define a specific seismological model for the country. Equations 13 and 14 allow the calculation of the theoretical Fourier amplitude spectrum, as a function of the seismic moment and the hypocentral distance.

Although, it is assumed that the media is homogeneous and isotropic, and that the dislocations occur instantly, these assumptions can be evaluated in the future. The heterogeneity of the earth's crust can be simulated using a stratified crust model (as, for example, the well-known Gutenberg model), which requires the use of ray theory to consider the waves reflection-refraction phenomena as they propagate through different media. Moreover, the time that the dislocation takes can be simulated using a dislocation function, as those proposed by Bernard et al. (1996), Hisada (2001) and Gallovic and

Brokesova (2004). These types of modifications, which could influence the mathematical definition of the Fourier amplitude spectrum, are additional aspects to consider in the future of this research.

5. STOCHASTIC SIMULATION

After defining the theoretical Fourier amplitude spectrum that generates, in the observer's location, a specific sub-source, the stochastic simulation of the associated accelerogram is performed. Following the methodology proposed by Boore (1983), the theoretical Fourier spectrum is multiplied by the amplitude spectrum derived from a gaussian noise signal. This creates a Fourier spectrum with defined amplitude and phase (i.e. in its complex representation), which can be converted to an accelerogram using the inverse Fourier transformation. To obtain better results, Boore (1983) suggested to modify the resulting signal by a shape function such as:

$$w(t) = at^b e^{-ct} H(t) \tag{15}$$

where *H(t)* is the unit step function. Constants *a, b* and *c* can be defined as:

$$a = \left(e/\varepsilon T_w\right)^b; \quad b = -\varepsilon \ln \eta / \left[1 + \varepsilon(\ln \varepsilon - 1)\right]; \quad c = b/\varepsilon T_w \tag{16}$$

where ε and η are the time to the peak of the shape function and the amplitude fraction at time T_w, respectively. In this work, the values suggested by Boore (1983) are used: $\varepsilon = 0.2$ and $\eta = 0.05$. T_w is the specified duration for the shape function (not necessarily the same duration of the accelerogram). Boore (1983) recommends setting $T_w = 2T_d$. The intense phase duration T_d, can be established following Herrman (1985) as:

$$T_d = \frac{1}{f_c} + 0.05R_i \tag{17}$$

The stochastic simulation allows the generation of accelerograms totally compatible with the theoretical formulation of the Fourier spectrum (integral approach). The methodology simulates low-frequencies in a proper way and randomly simulates high-frequencies, resulting in coherent acceleration signals that are satisfactorily defined for engineering purposes.

6. ACCELEROGRAM INTEGRATION

After the accelerograms are calculated for earthquakes related to each sub-source (i.e. the earthquakes generated with a portion of the total seismic moment), these are added in the observer's site as independent contributions from each sub-source. Each sub-source contributes to the observer's site with a different accelerogram, all of which have different arrival times. This is an imperative condition, especially in near-field problems, where the distance to the observer is in the same (or less) order to the rupture's size. The accelerogram's arrival time (t_i) is defines as:

$$t_i = \frac{R_i}{\beta} \tag{18}$$

Even though this is a simplistic approach, general results seem to be appropriate. Better estimates can be obtained by applying ray theory to establish arrival times within a stratified crust media.

The resulting accelerograms are added in the observer's site assuming the arrival times estimated previously. The outcome is a total acceleration signal that integrates, with the corresponding lags, the contributions of all the sub-sources. This addition is not totally coherent (which is the main issue with composite approaches, therefore, it is also ours); consequently, to maintain a radiated spectrum ω^{-2} a correction must be included in the final accelerogram. A ω^{-2} filter is applied in the accelerogram, defined by the corner frequency estimated with the total seismic moment (note that the filter corresponds to the source's scaling factor (S) introduced in equation 9, and normalized by its maximum amplitude (S_{Max})):

$$H(f) = \frac{1}{S_{Max}} \cdot \frac{M_0 \cdot f^2}{1 + \left(\frac{f}{f_c} \right)^2} \tag{19}$$

This method can be applied to any seismic source in any territory. It requires a geometric model of the source, the moment magnitude, the location of the hypocenter (in the x, y, z coordinated system defined here), and the observer's location (calculation site). This method was implemented in the software Strong Motion Analyst (Bernal 2014), available free of charge prior communication with the author. To illustrate the results obtained with this methodology, a model was defined as seen in Table 1. The coordinated system x, y, z was conveniently defined to match the epicenter coordinates. The observer's location was established in the same location as the epicenter, to force the occurrence of a finite-source problem.

Table 1. Source model parameters

Magnitude	M_w	7
	M_0	3.55E+26
Hypocenter	x	0
	y	0
	z	30 Km
Fault orientation	ϕ_s (strike)	45
	δ (dip)	45
	λ (rake)	0
Sub-sources	N (side) (Ec. 3)	81
	Total sub-sources (N^2)	6561
	M_{0i}	5.41E+22
	M_{wi}	4.46

As seen in Table 1, the simulated accelerogram for a 7-magnitude earthquake, following the problem conditions, is equivalent to a corrected integration of 6561 earthquakes of magnitude 4.46. Figure 3 presents the resulting accelerogram. The Fourier amplitude spectrum and the accelerogram response spectrum are presented in Figure 4. Figure 5 shows the resulting accelerograms for 5 additional simulations performed for the same source parameter configuration as shown in Table 1.

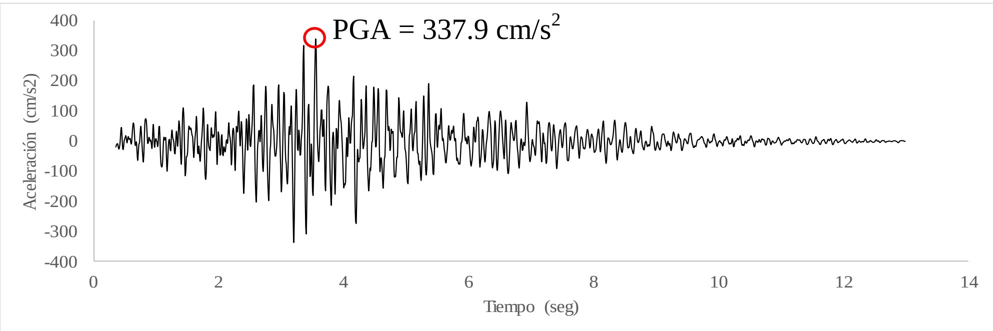

Figure 3. Synthetic accelerogram resulting from an earthquake of magnitude 7, with hypocenter at a depth of 30 Km. The observer's site corresponds to the epicenter. The source model parameters are shown in Table 1.

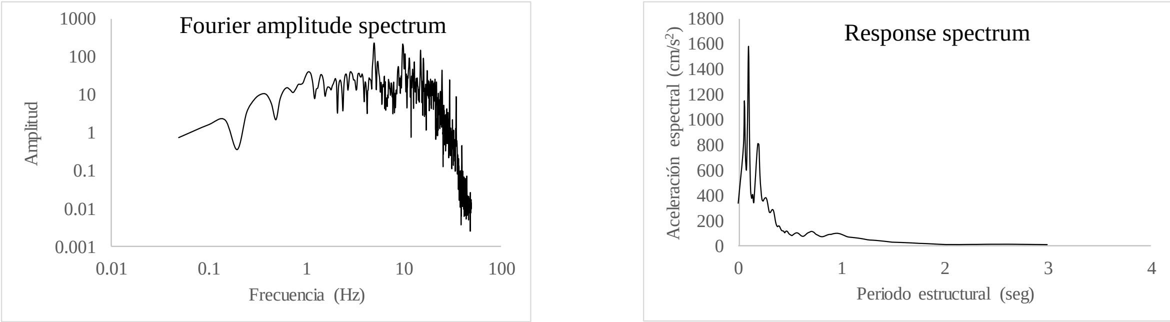

Figure 4. Fourier amplitude spectrum and response spectrum obtained from the simulated accelerogram.

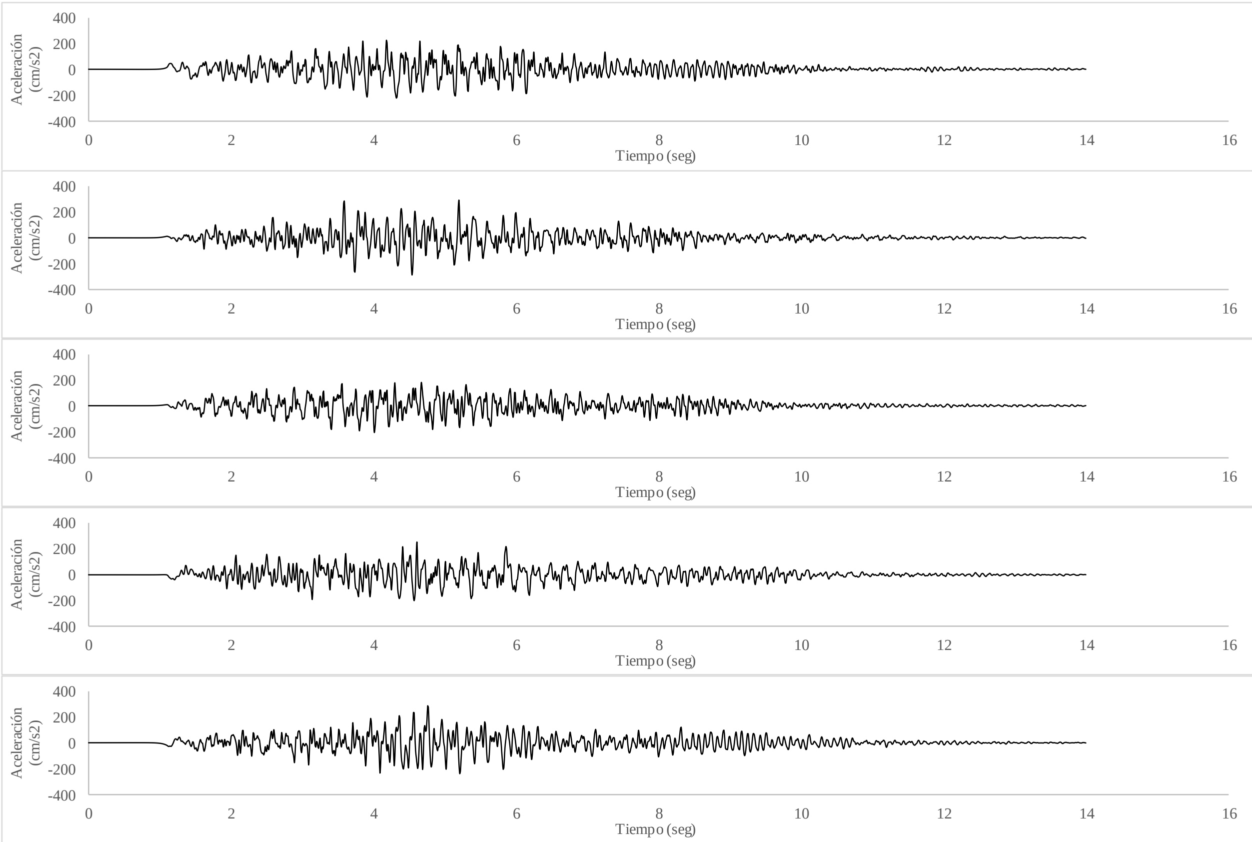

Figure 5. Five simulations of the accelerogram generated after the model parameters presented in Table 1.

7. CONCLUSIONS

The presented methodology calculates accelerograms from the definition of a hybrid source model, by the combination of multiple approaches widely used in seismology and earthquake engineering practice. The hybrid source model is based on the definition of the rupture zone as a function of the total seismic moment of the earthquake, which is subdivided in a convenient way to make the use of point source models and stochastic simulations suitable for application. The result is a collection of accelerograms that are integrated in the observer's site, considering the arrival times corresponding to the hypocentral distances of each sub-source. The resulting accelerogram is corrected by a ω^{-2} filter to maintain a coherent result. The model outcomes are sufficiently good for engineering applications related to hazard assessment, microzonation, risk assessment and structural calculation. Possible improvements to the model are detailed throughout the paper.

The accelerogram simulation is a research field with multiple potential applications. In relation to hazard assessments, accelerogram simulation allows the calculation of any strong motion intensity magnitude because they are derived from the accelerogram. This sets an important difference with the traditional method to estimate seismic hazard using attenuation functions. Although, classic attenuation models are generalized, and appropriate for national and regional assessments, local hazard modeling can benefit from simulated accelerograms. The combination of a hazard model based on simulated accelerograms with integral models of site response, like the one proposed by Bernal (2014) and currently applied in Bogotá (Bernal et al. 2017) and in Manizales (Bernal 2015), would provide state-of-the-art seismic microzonation studies. This would provide time-dependent strong motion estimates that are coherent from the occurrence of the earthquakes to the arrival of seismic waves to the structure's foundations.

Moreover, seismic risk assessment is a research field that can be improved by considering a collection of seismic scenarios, not limited to the distribution of few strong motion parameters (as it is the current common practice), but considering the spatial distribution of the accelerograms generated by each event included in the loss assessment. The proposed model can be applied in risk assessment with the introduction of advanced vulnerability models, like the ones related to the definition of buildings as a compound system (structural system, non-structural components and contents), which can be affected by a specific seismic demand. In these type of models, the vulnerability of each component is characterized by a loss function that states the variability of the probability moments of the economic loss (expected value and variance) of an element subjected to the seismic demand transmitted by the structure. The seismic demand of each structure element is estimated using a collection of transference functions that relate the strong motion input, in the building base, with seismic parameters relevant to each element inside the building.

Finally, an important application of accelerograms simulation is the risk-based seismic resistant design; appropriate for essential buildings and infrastructure components. In the risk-based design, it is important to establish the stresses and deformations, in the structure's elastic and inelastic range, for multiple seismic demands. With the proposed method, it is possible to define a collection of accelerograms, fully consistent with the regional seismotectonics, that collectively describe all the possible ways a strong motion can occur in the future location of the structure. By using time dependent structural response models, it is possible to establish damages and losses related to each of the considered earthquakes (individually represented by an accelerogram); and in this way, define the design level based on the tolerable risk according to the importance of the construction.

8. REFERENCES

Aki K (1967). Scaling Law of Seismic Spectrum. *Journal of Geophysical Research*, 72: 1217-1231.

Aki K, Richards PG (2002). Quantitative Seismology, 2nd Ed. *University Science Books*, Sausalito, CA.

Atkinson GM (1995). Attenuation and Source Parameters of Earthquakes in the Cascadia Region. *Bull. Seism. Soc. Am*, 85(5): 1327-1342

Bernal GA (2014). Metodología para la modelación, cálculo y calibración de parámetros de la amenaza sísmica para la evaluación probabilista del riesgo. *PhD Dissertation, Universitat Politecnica de Catalunya*.

Bernal GA (2014). Strong Motion Analyst. Seismic data processing software.

Bernal GA, Cardona OD (2015). Calibración de funciones de atenuación basadas en el espectro de fuente radiado y su aplicación en Colombia. En: Barbat AH (ed.): *Monografías de Ingeniería Símica*. CIMNE, UPC, Barcelona.

Bernal GA, Zuloaga D, Cardona OD (2017). Modelo probabilista de respuesta sísmica de los suelos de Bogotá. *VII Congreso Nacional de Ingeniería Sísmica.* AIS, Colombia

Bernard P, Herrero A, Berge C (1996). Modeling Directivity of Heterogeneous Earthquake Ruptures, *Bulletin of the Seismologmal Society of America*. 86: 1149–1160.

Boore D (1983). Stochastic simulation of high-frequency ground motions based on seismological models of the radiated spectrum. *Bulletin of the Seismologmal Society of America*. 73(6): 1865-1894.

Brune JN (1970). Tectonic Stress and the Spectrum of Seismic S Waves from Earth. *Journal of Geophysical Research*, 75: 4997-5009.

Castro RR, Anderson JG, Singh SK (1990). Site response, attenuation and source spectrum of S waves along the Guerrero, Mexico, subduction zone. *Bulletin of the Seismologmal Society of America*. 80(6): 1481-1503

Gallovic F, Brokesova J (2004). On strong ground motion synthesis with k^{-2} slip distributions. *Journal of Seismology*. 8:211.

Gallovic F, Brokesova J (2007). Hybrid k-squared source model for strong ground motion simulations: Introduction. *Physics of the Earth and Planetary Interiors*. 160: 34–50.

Hanks TC, Kanamori H (1979). A moment magnitude scale. *Journal of Geophysical Ressearch*. 84: 2348–2350.

Hanks TC (1982). fmax. *Bulletin of the Seismologmal Society of America*. 72(6): 1867-187

Hassani B, Zafarani H, Farjoodi J, Ansari A (2011). Estimation of site amplification, attenuation and source spectrum of S-waves in the East-Central Iran. *Soil Dynamics and Earthquake Engineering* 31: 1397–1413

Hermann RB (1985). An extension of random vibration theory estimates of strong ground motion to large distances, *Bulletin of the Seismologmal Society of America*. 73: 157-171.

Hisada Y (2001). A Theoretical Omega-Square Model Considering the Spatial Vari- ation in Slip and Rupture Velocity. Part 2: Case for a Two-Dimensional Source 16 Model, *Bulletin of the Seismologmal Society of America*. 91:651–666.

Knopoff L (1964). Q. *Review of Geophysics*, 2: 625-660.

Mai P, Beroza G (2003). A hybrid method for calculating near-source, broadband seismograms: application to strong motion prediction. *Physics of the Earth and Planetary Interiors* 137: 183–199.

Ordaz M, Singh SK (1992). Source spectrum and spectruml attenuation of seismic waves from Mexican earthquakes, and evidence of amplification in the hill zone of Mexico City. *Bulletin of the Seismologmal Society of America*. 82 (1): 24-43

Özel NM, Harmandar E, Pinar A (2011). Sensitivity of the strong ground motion time histories to a finite source model: A case study for the January 12, 2010 Haiti earthquake (Mw=7.0). *Soil Dynamics and Earthquake Engineering*. 31: 1441–1451.

Singh SK, Bazan E, Esteva L (1980). Expected earthquake magnitude from a fault, *Bulletin of the Seismologmal Society of America*. 70:903-914.

Singh SK, Iglesias A, García D, Pacheco JF, Ordaz M (2007). Q of Lg Waves in the Central Mexican Volcanic Belt. *Bulletin of the Seismologmal Society of America*. 97(4): 1259–1266

Tavakoli B, Pezeshk S (2005). Empirical-Stochastic Ground-Motion Prediction for Eastern North America. *Bulletin of the Seismologmal Society of America*. 95(6): 2283–2296